

Is it possible to grow amorphous normal nanosprings ?

Alexandre F. Fonseca^{1‡}, C. P. Malta¹ and D. S. Galvão²

¹ Instituto de Física, Universidade de São Paulo, Caixa Postal 66318, 05315-970, São Paulo, Brazil

² Instituto de Física ‘Gleb Wataghin’, Universidade Estadual de Campinas, Unicamp 13083-970, Campinas, SP, Brazil

E-mail: afonseca@if.usp.br, coraci@if.usp.br, galvao@ifi.unicamp.br

Abstract.

Nanosprings have been object of intense investigations in recent years. They can be classified as *normal* or *binormal* depending on the geometry of their cross-section. *Normal* amorphous nanosprings have not been observed experimentally up to now so we have decided to investigate into this matter. We discuss the shape of the catalyst in terms of the cross-sectional shape of the nanospring, and show that, within the vapor-liquid-solid model, the growth of amorphous *binormal* nanosprings is energetically favoured.

PACS numbers: 81.07.-b, 62.25.+g, 81.16.Hc

Submitted to: *Nanotechnology*

‡ Present address: Alan McDiarmid Nanotech Institute, University of Texas at Dallas, Richardson, TX 75083-0688, USA.

1. Introduction

There exist various methods and processes for growing nanostructures. Different types of nanostructures require different methods and processes to be grown. Several groups are working on the development and improvement of the growth processes motivated not only by new physical phenomena but also by the great variety of technological applications [1–9].

In particular, the existence of helically shaped nanowires (nanosprings or nanohelices) is of great interest because of the potential applications in nanoelectronics, nanomechanics and nanoelectromechanical systems [10]. Examples of such structures are quasi-nanosprings [11], helical crystalline nanowires [12–15], and amorphous nanosprings [16–21].

In contrast to the formation of straight nanowires, the synthesis of helical nanostructures requires either the existence of anisotropy at some level of the growth process, or the existence of external forces holding the nanowire into a helical shape. Both cases have been reported in the literature. In the case of amorphous nanosprings, McIlroy *et al* [10, 16] have shown, based on the vapor-liquid-solid (VLS) growth model [22], that the anisotropy in the contact angle between the catalyst and the nanowire induces helical growth. In the case of crystalline nanosprings, Kong and Wang [14] reported the formation of nanohelices of zinc oxide (ZnO) and showed that the electrostatic interaction between the nanowire, and the substrate where it is grown, holds the ZnO nanowires in a helical shape.

A helical structure is classified as *normal/binormal* depending on the orientation of its cross-section with respect to the *normal* or *binormal* vectors [23, 24]. We have analyzed nanosprings of various materials, reported in the literature [14–18], and have not found a single case of *normal* amorphous nanohelices. In the case of crystalline helical nanostructure, Gao *et al* [26] have recently reported the synthesis of a ZnO *normal* nanohelix. Why normal amorphous nanosprings have not been observed ? Using the VLS model we provide the first theoretical explanation for the non-existence of amorphous *normal* nanohelices. We have extended the VLS growth model [10, 16], so as to take into account possible asymmetries in the shape of the catalytic particle. We show that the growth of amorphous *binormal* nanosprings is energetically more favoured in comparison to the growth of *normal* ones.

Normal and *binormal* helical nanostructures may lead to different technological applications. We have shown that two nanosprings of same radius and pitch, same material, possessing the same cross-section geometry, but differing by the fact that one is a *normal* helical structure and the other is *binormal*, have different stiffness [24, 25]. In this comparison, the *normal* nanospring is always stiffer than the *binormal* one [24, 25].

In Section 2, we briefly describe the geometry of a helical structure and give the definition of *normal* and *binormal* helices. The reported experimental results are classified according to this definition. In Section 3 we analyse the shape of the nanospring cross-sections and discuss the possible shapes of the catalytic particle necessary to drive

the growth of amorphous nanohelices with non-circular cross-section, through the VLS mechanism. In Section 4, based on the VLS growth model, we show that the growth of amorphous *binormal* nanospring is energetically favoured. In Section 5 we summarize our results and conclusions.

2. Nanosprings geometric features

A helical space curve is called *a curve of constant slope*, *i. e.*, a curve whose tangent lines make a constant angle with a fixed direction in the space (the helical axis) [27]. $\{\mathbf{n}, \mathbf{b}, \mathbf{t}\}$ is a frame, called *Frenet basis*, which is a right-handed orthonormal basis defined at each point along a space curve, where \mathbf{t} is the tangent unit vector, \mathbf{n} is the *normal* unit vector and \mathbf{b} is the *binormal* unit vector. In order to define the *normal* and *binormal* vectors we consider the plane defined by the points P_1 , P_2 and P_3 belonging to the space curve. In the limit where P_2 and P_3 approach P_1 , the plane is called the *osculating plane* of the curve at P_1 [27]. The tangent vector \mathbf{t} belongs to the osculating plane. \mathbf{n} is defined as the unit vector perpendicular to \mathbf{t} , that lies in the osculating plane while \mathbf{b} is defined as the unit vector perpendicular to \mathbf{t} , that is perpendicular to the osculating plane.

Let I_1 and I_2 be the principal moments of inertia of the cross-section of a rod, along the two principal axes of the cross-section. Along this paper, cross-sections of rods with $I_1 = I_2$ will be called *symmetric cross-sections* and cross-sections of rods with $I_1 \neq I_2$ will be called *asymmetric cross-sections*. According to this definition, circular and squared cross-sections are symmetric, while elliptic and rectangular cross-sections are asymmetric.

Given a rod with asymmetric cross-section, we define the unit vector \mathbf{d} lying in the cross-section plane along the direction of the largest bending stiffness (it is the direction of the larger semiaxis of an elliptic cross-section). The helical structure is said to be *normal* (*binormal*) if \mathbf{d} is in the direction of the unit vector \mathbf{n} (\mathbf{b}). In the case of a rod with symmetric cross-section, the *normal* and *binormal* structures degenerate into one type of helix that we called a *neutral helix*. Figure 1 displays examples of *neutral*, *normal* and *binormal* helices, with the shape of their corresponding cross-section.

Inspection of the transmission electron microscopy (TEM) images of the amorphous nanosprings reported in Refs. [10, 16–18] shows that all of them are either *neutral* (Fig. 1a) or *binormal* (Fig. 1c) helices, and none of them is a *normal* helix (Fig. 1b).

The silicon carbide (SiC) nanospring reported in Ref. [18] can be classified as a neutral helix. According to Ref. [18], this nanospring is formed from a nanowire with circular cross-section. The TEM image of the boron carbide (BC) nanospring depicted in panel b) of Figure 10 of Ref. [10] is also a neutral helix grown from a nanowire of circular cross-section.

The reported SiC [10], BC [16], and silicon oxide (SiO_2) [17] nanosprings are clearly examples of *binormal* helices. According to Ref. [17], the SiO_2 nanospring was grown from a non-cylindrical nanowire. The reported SiC and BC *binormal* nanosprings were formed from a nanowire with rectangular cross-section [10, 16].

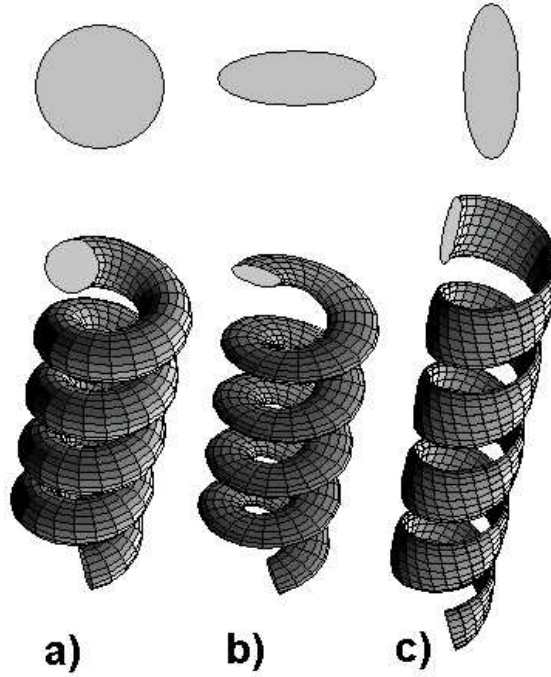


Figure 1. a) *Neutral* helix made of a rod with circular cross section, b) *normal* and c) *binormal* helices made of a rod with an asymmetric cross-section. The cross-section shape is depicted above the corresponding helix type.

To our knowledge, the only *normal* helical nanostructure reported in the literature is the crystalline ZnO nanohelix synthesized by Sb induced thermal evaporation [26]. The scanning electron microscopy (SEM) images of these ZnO nanohelices show that each helical period is formed by the sequence of six straight blocks, each block growing in a given crystalline direction.

As up to now experimentalists have not reported the growth of amorphous nanosprings of the *normal* type, we here present the results of our investigation towards answering the question: *is it possible to grow amorphous nanosprings of the normal type ?*

According to our previous analysis [24, 28], amorphous nanosprings grown by the VLS mechanism are dynamically stable. This stability stems from the intrinsic curvature produced by the catalytic particle in the forming nanospring. The *intrinsic curvature* of a rod represents its tridimensional shape when it is free from external stresses. Goriely and Shipman have studied the dynamical stability of *normal* and *binormal* helices [23] and showed that intrinsically *normal* or *binormal* helical filaments are always stable. Therefore, from the mechanical point of view, and in agreement with our previous analysis [24, 28], there is no mechanical prohibition for the existence of an amorphous *normal* nanospring, thus both types of helical amorphous nanostructures could be produced by the usual VLS mechanism. We have conjectured that the shape of the liquid catalyst is the key to explain the absence of normal amorphous nanospring. Thus

we have extended the VLS growth model to address also the case of non-spherical liquid catalyst.

3. The VLS model with non-spherical catalyst

According to the VLS growth model, a liquid droplet of metal absorbs the material from the surrounding vapor, and after super-saturation of the absorbed material within the droplet, the excess material precipitates at the liquid-solid interface forming the nanowire beneath the metallic catalyst. The model is based on the interaction between the surface tension of the liquid-vapor (γ_{LV}), solid-vapor (γ_{SV}) and solid-liquid (γ_{SL}) interfaces. McIlroy *et al* [10, 16] proposed that the helical growth process occurs due to a contact angle anisotropy (CAA) at the catalyst-nanowire interface. The trajectory of the metallic catalyst is driven by the work needed to shear it from the surface of the nanowire. This work is called the thermodynamic work of adhesion W_A and can be computed in terms of the surface tensions by [10]:

$$\begin{aligned} W_A &= \gamma_{SV} + \gamma_{SL} - \gamma_{LV} \\ &= \gamma_{SV}(1 - \cos \theta) \end{aligned} \quad (1)$$

where θ is the angle between the surface tensions γ_{SL} and γ_{SV} . Figure 2 reproduces the schematic diagram of a spherical catalyst placed asymmetrically on the nanowire, in accordance to the McIlroy *et al* modified VLS growth model [10].

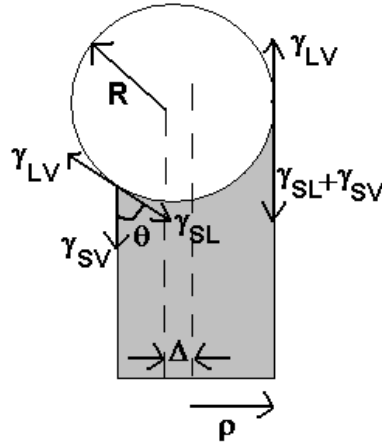


Figure 2. Schematic diagram of the catalytic particle of radius R atop a nanowire of radius ρ , whose center is shifted of Δ with respect to the axis of the nanowire.

Figures 1b) and 1c) display the cross-section of *normal* and *binormal* helical structures, respectively. We can see in these figures that, with respect to the plane of the page, the cross-section of the *normal* helix has a horizontal dimension larger than the vertical one, and vice-versa for the *binormal* helix. The nanowire grows from the deposition of the material absorbed by the liquid catalyst, so that, to grow structures with asymmetric cross-section, the surface of contact between the catalytic particle and the nanowire must follow the shape pattern of the cross-section.

An increase of the diameter of the spherical catalyst in the anisotropic position with respect to the nanowire axis (as in Fig. 2), without increasing the nanowire diameter, increases the asymmetry of the surface of contact between the catalyst and the nanowire. However, according to McIlroy *et al* [10, 16], if the diameter of the spherical catalyst increases systematically, so that Δ/R decreases (see Fig. 2), the CAA becomes less significant and the work of adhesion becomes equal to that of the symmetric configuration in which the nanowire grows linearly.

Therefore, to have the surface of contact between the catalyst and the nanowire following the pattern of a nanospring of asymmetric cross-section, in the model considered by McIlroy *et al* [10, 16] (see Fig. 2) we allow the catalyst to possess a non-spherical shape. To produce a *normal* (*binormal*) amorphous nanospring of elliptic cross-section, as Fig. 1b) (Fig. 1c)) we propose that the catalytic particle is an ellipsoid as displayed in Fig. 3a) (Fig. 3b)). The growth of an asymmetric nanospring, that is driven by an elliptic catalyst, as shown in Fig. 3, is obtained in the same way as that driven by a spherical catalyst (Fig. 2): the growth rate velocity is larger at the interface where the work of adhesion is smaller [10, 16]. Of course, in the case of growth of an asymmetric nanospring the shape of the interface of contact between the catalyst and the nanowire is not circular.

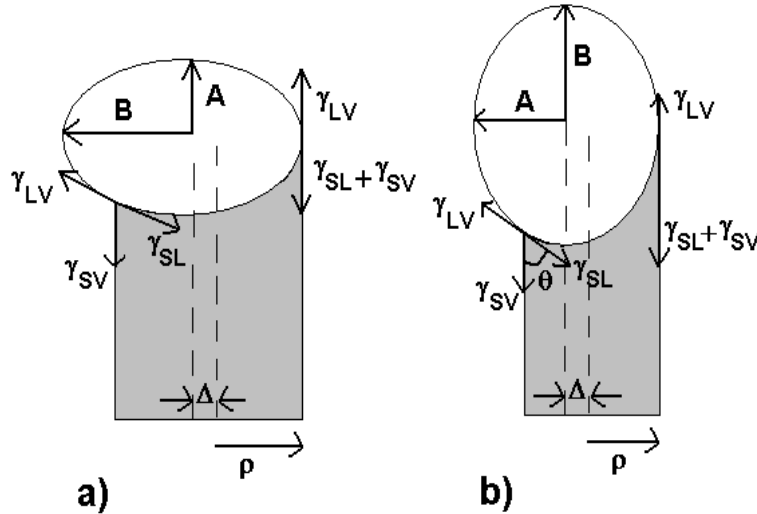


Figure 3. Schematic diagrams for the growth of a) *normal* and b) *binormal* nanosprings of elliptic cross-section. The center of the elliptic catalyst is shifted of Δ with respect to the axis of the nanowire. ρ is the radius of the nanowire, and $A < B$ are the semi-axes of the elliptical catalyst in the plane of the figure.

The TEM images of the transition regions from the linear nanowire growth to nanospring growth (Figs. 15 and 17 of Ref. [10], Fig. 2 of Ref. [16], Fig. 5 of Ref. [18] and Fig. 3a of Ref. [17]) give support to our proposal. All of these figures display remnants of the catalyst inside the transition region. In Ref. [10] these remnants are assumed to have spherical shape. However, a minucious examination of these remnants shows that some of them are not spherical. Fig. 3a of Ref. [17] presents an oval-shaped particle inside the

transition region. Fig. 15b of Ref. [10] or Fig. 2b of Ref. [16] shows that the part of the catalyst lying inside the nanowire in the transition region is approximately elliptic. The shape of the particle inside the transition from linear to helical SiC nanowire displayed in Fig. 5 of Ref. [18] has a more complex shape.

According to McIlroy *et al* [10], changes in the materials absorbed by the catalyst, the introduction of additional elements, and changes in the local temperature can introduce imbalances in the energy related to the surface tension of the liquid-vapor (γ_{LV}), solid-vapor (γ_{SV}) and solid-liquid (γ_{SL}) interfaces, that lead to variations in the shape and mass of the catalyst during the growth process of the nanowire.

Therefore, we propose that after the transition from linear to helical growth of the nanowire, the ejected part of the catalyst has to possess an asymmetric shape to drive the growth of a nanospring with asymmetric cross-section.

4. Why amorphous *normal* nanosprings have not been observed ?

The idea of considering non-spherical catalyst is essential for explaining the formation of a nanospring with asymmetric cross-section. Now, to explain why amorphous *normal* nanosprings have not been synthesized we have to look into the Contact Angle Anisotropy (CAA) [10,16]. According to McIlroy *et al* proposal [10,16], the CAA has to be significant for the helical growth of a nanowire. So, if the CAA is significant for the growth of *normal* and *binormal* nanosprings, then both types of nanosprings could be grown through the VLS mechanism. To explain the absence of amorphous *normal* nanosprings, we shall analyse the significance of the CAA for growing *normal* (Fig. 3a)) and *binormal* (Fig. 3b)) nanosprings.

According to McIlroy *et al* [10,16], if the diameter of the spherical catalyst increases systematically, so that Δ/R decreases (see Fig. 2), the CAA becomes less significant and the work of adhesion becomes equal to that of the symmetric configuration in which the nanowire grows linearly. As we are dealing with non-spherical catalyst we propose that the significance of the CAA comes from the ratio Δ/X , where X is the dimension of the catalyst particle along the direction of the shift of the catalyst with respect to the nanowire axis. In the case of a spherical catalyst of radius R , $X = R$, giving McIlroy *et al* [10,16] ratio Δ/R , while in the case of an elliptical catalyst $X = B$ ($X = A$) in the scheme depicted in Fig. 3a) (Fig. 3b)).

We shall analyze the significance of the CAA for both cases depicted in Fig. 3. The magnitude of B (A) will determine the significance of the CAA for the scheme depicted in Fig. 3a) (Fig. 3b)). Since Δ/B is always smaller than Δ/A , we expect that the scheme displayed in Fig. 3a) is less favourable for growing a helical nanowire than that of Fig. 3b). To show this, we have calculated the work of adhesion along the interface solid-liquid-vapor of an elliptical metallic catalyst in contact with the nanowire, for the two situations depicted in Fig. 3.

Fig. 4 displays the work of adhesion W_A for growing a helical nanostructure, driven by an elliptical catalyst having dimensions $A = 1.5$, $B = 2.0$, onto a nanowire with

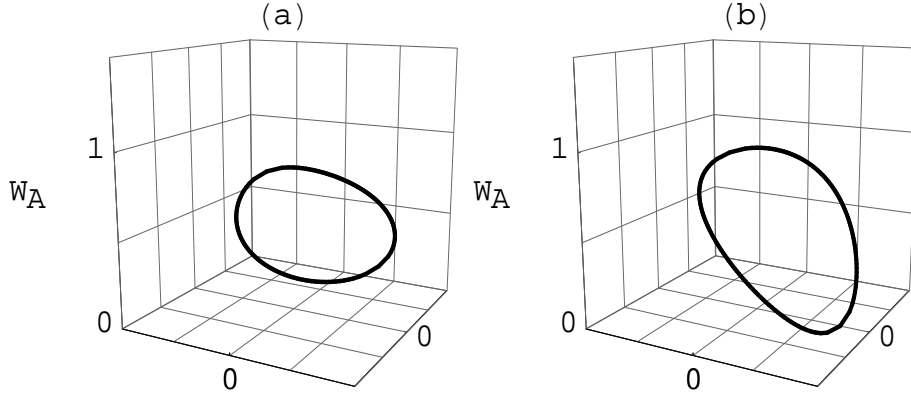


Figure 4. The work of adhesion W_A (in arbitrary units) along the interface solid-liquid-vapor formed by an elliptic catalytic particle ($A = 1.5, B = 2.0$) onto a nanowire of $\rho = 1.0$, with $\Delta = 0.5$, for (a) *normal* growth, depicted in Fig. 3a), and (b) *binormal* growth, depicted in Fig. 3b).

$\rho = 1.0$, and $\Delta = 0.5$ (see Fig. 3). The condition for the optimal geometry to promoting helical growth has been inferred from that obtained by McIlroy *et al* [16] for the growth of a helical nanowire in the case of a spherical catalyst. They found that $R/\rho \simeq 1.5$ [10, 16]. As the catalyst here has elliptic shape, we propose to replace R by X , so that the condition for the optimal geometry to promoting helical growth can be written as $X/\rho \simeq 1.5$. The chosen values of ρ and Δ are such that the significance of the CAA gives the optimal geometry for the promotion of helical growth in the case of spherical catalyst [16] with radius $R = 1.5$. Panel (a) of Fig. 4 shows the work of adhesion for the scheme of Fig. 3a) for growing a *normal* nanospring ($(X/\rho) = (B/\rho) = 2.0$). Panel (b) of Fig. 4 shows the work of adhesion for the scheme of Fig. 3b) for growing a *binormal* nanospring ($(X/\rho) = (A/\rho) = 1.5$). The difference between the minimum and the maximum values of the work of adhesion, hereafter called d_{WA} , gives a measure of the amount of anisotropy in the contact angle and, therefore, the CAA significance for growing a helical nanostructure in that situation. $d_{WA} = 0.458$ for the case displayed in the Fig. 4a) while $d_{WA} = 0.922$ for the case displayed in the Fig. 4b), thus indicating that for the elliptic catalytic particle having dimensions $A = 1.5, B = 2.0$, the optimal geometry to promoting helical growth corresponds to the *binormal* nanohelix for which $(X/\rho) = (A/\rho) = 1.5$.

To show that the larger the value of Δ/X , the smaller the significance of the CAA in the helical growth, we have calculated d_{WA} keeping B fixed and varying A , using the parameters of Fig. 4 ($\rho = 1.0, \Delta = 0.5$). We have considered three fixed values of B : (i) $B = 2.0$ and $B = 3.0$ for the growth scheme in Fig. 3b); (ii) $B = 1.5$ for the growth scheme in Fig. 3a). To consider only catalysts for which their extreme edges coincide with the extreme edge of the nanowire, as considered by McIlroy *et al* [16] (see Fig. 2 or 3), we only calculate the d_{WA} for $X \geq (\rho + \Delta)$ (in this case $\rho + \Delta = 1.5$). So, in the case

of the growth scheme in Fig. 3b), for which $X = A$, we have varied $A \in [1.5, 9.0]$ for both values of fixed B . In the case of the growth scheme in Fig. 3a) (for which $X = B$) we have fixed $B = 1.5$, and varied $A \in [0.75, 3.30]$.

The $d_{WA} \times A$ plotting for the cases $B = 3.0$, $B = 2.0$, and growth scheme in Fig. 3b), are displayed in Figs. 5a) and 5b), respectively. Notice that for $A < B$ ($A > B$) the nanohelix is *binormal* (*normal*) and it is neutral for $A = B$ (case of spherical catalyst). Fig. 5 shows that d_{WA} exhibits a small peak at $A = B$, but for all other values of A it decreases as A increases, implying that the significance of CAA decreases as Δ/A decreases. The significance of CAA is larger for $A = 1.5$ therefore it corresponds to the optimal geometry to promoting helical growth corroborating our proposal of replacing the condition $R/\rho \simeq 1.5$ by $X/\rho \simeq 1.5$ ($X = A$ for the growth scheme in Fig. 3b)). The

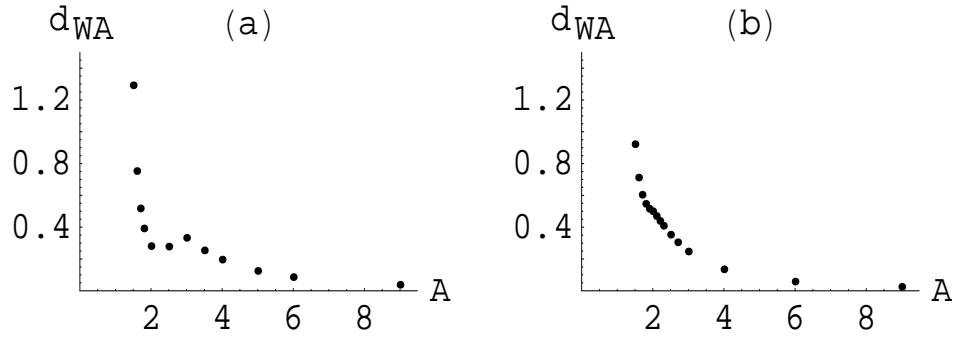


Figure 5. The difference, d_{WA} (in arbitrary units), between the minimum and the maximum values of the work of adhesion as a function of $A \in [1.5, 9.0]$, for the scheme depicted in Fig. 3b), with $\rho = 1.0$ and $\Delta = 0.5$. B is fixed: a) $B = 3.0$; b) $B = 2.0$.

$d_{WA} \times A$ plotting for the case $B = 1.5$, and growth scheme in Fig. 3a), is displayed in Fig. 6 (bottom), for $A \in [0.75, 3.30]$. In this case $X = B$, and according to our proposal the condition for the optimal geometry to promoting helical growth is always satisfied since $(X/\rho) = (B/\rho) = 1.5$. The case of spherical catalyst, $A = B = 1.5$, corresponds to the optimal geometry to promoting helical growth according to McIlroy *et al* [16]. Notice that for $A < B = 1.5$ ($A > B = 1.5$) the nanohelix is *normal* (*binormal*), and it is neutral for $A = 1.5$ (this corresponds to the case of spherical catalyst). Fig. 6 (bottom) shows that d_{WA} is decreasing for $A < B$, while for $A > B$ it is increasing (at a faster rate). At the top of Fig. 6 we display the work of adhesion along the interface solid-liquid-vapor formed by the elliptic catalytic particle onto the nanowire for the cases $A = 1.13$ (top left) and $A = 2.00$ (top right), the latter case being the same one displayed in Fig. 4b). $d_{WA} = 0.922$ for the case $A = 2.00$ (Fig. 6, top right), and $d_{WA} = 0.743$ for the case $A = 1.13$ (Fig. 6, top left). In these two cases the elliptic catalyst has its major axis approximately 1.33 times its minor axis, and our results indicate that the *binormal* type is favoured energetically.

From the $d_{WA} \times A$ plottings in Figs. 5 and 6, we conclude that the growth of a *binormal nanospring* is favoured energetically whenever both semiaxes of the elliptic

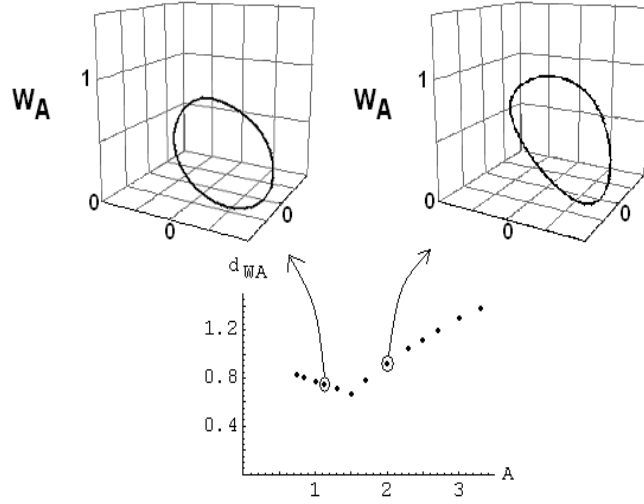


Figure 6. Bottom: the difference, d_{WA} (in arbitrary units), between the minimum and the maximum values of the work of adhesion as a function of $A \in [0.75, 3.30]$, for $B = 1.5$ fixed, $\rho = 1.0$ and $\Delta = 0.5$, for the scheme depicted in Fig. 3a). Notice that the nanohelix is *normal* (*binormal*) for $A < 1.5$ ($A > 1.5$). Top left (top right) is the work of adhesion, in arbitrary units, along the interface solid-liquid-vapor formed by the catalytic particle, with $A = 1.13$ ($A = 2.00$), onto the nanowire with the parameters above (they correspond to the points encircled in the $d_{WA} \times A$ plotting).

catalyst are $\geq (\rho + \Delta)$. If the major semiaxis is $\geq (\rho + \Delta)$ while the minor semiaxis is $< (\rho + \Delta)$, then it is not possible to grow a *binormal nanospring*, and in this case it would be possible to grow a *normal nanospring* as indicated by the $d_{WA} \times A$ plotting in Fig. 6 when $A < 1.5$. So, depending on the dimensions of the elliptic catalyst relative to $(\rho + \Delta)$ the CAA may be significant for growing a *normal* nanohelix whenever $A < (\rho + \Delta)$ (see Fig. 3).

In the particular case of $B \simeq A$, the grown helix could be either *normal* or *binormal* as shown in the $d_{WA} \times A$ plottings (Figs. 5 and 6) within the region around $B = A$. However, in this case, the shape of the catalyst is approximately spherical, and the resulting helical structure will be very similar to that of a *neutral* helix (spherical catalyst). Therefore, *normal* or *binormal* nanosprings grown by an almost spherical catalyst are not experimentally distinguishable from a *neutral* nanospring.

The TEM images of the transition regions from the linear nanowire growth to nanospring growth reported in the literature (Figs. 15 and 17 of Ref. [10], Fig. 2 of Ref. [16], Fig. 5 of Ref. [18] and Fig. 3a of Ref. [17]), show that the remnant frozen part of the catalyst is not spherical. This fact, together with our results in Figs. 5 and 6, allows us to infer that the part of the catalyst that was ejected, and drove the helical growth, had the elliptic shape displayed in Fig. 3b).

The formation of helical nanowires of rectangular cross-section, as the amorphous BC nanospring displayed in Figure 1 of Ref. [16] or the amorphous SiC nanospring displayed in Figure 13 of Ref. [10], can be explained using our extended VLS growth

model for a rectangular metallic catalyst. If the smaller side of the rectangular catalyst is not larger than the displacement Δ , the CAA is significant and the helical growth can occur.

5. Conclusions

We have studied the geometric features of several types of nanosprings reported in the literature. The published images of several nanosprings and nanohelices were analyzed and we have verified the non-existence of one type of helical structure in the case of amorphous nanostructures: *normal nanohelix*. In the case of amorphous materials, we discussed the importance of the shape of the catalyst in order to drive the growth of a nanospring of asymmetric cross-section. We extended the modified VLS growth model to include non-spherical shapes of the catalyst so as to explain the growth of asymmetric amorphous nanosprings. The conformation of the amorphous nanosprings seen in the TEM images are explained by our proposal.

We have shown that the non-spherical shape of the metallic catalyst, within the model proposed by McIlroy *et al* [10, 16], can induce the growth of amorphous nanosprings with asymmetric cross-section. We have also shown that the anisotropy in the work of adhesion along the interface liquid-solid is more significant for growing a *binormal nanohelix* than for growing a *normal nanohelix*, thus explaining the absence of amorphous *normal* nanosprings.

From the present study we conclude that the resulting type of helical nanostructure (its cross-section) is related to the shape of the metallic catalyst that induced its growth. So, from the type and shape of the nanospring it is possible to qualitatively infer the shape of the metallic catalyst. For example, if the period of the turns changes along the nanospring, as seen in the SiO₂ nanosprings of Ref. [17], our analysis suggests that the size and shape of the catalyst must have changed during the nanospring formation.

Our results are in perfect agreement with the experimental TEM images of various nanosprings and provide new insight on the geometric and mechanical characteristics of both types of helices. It is well established that for some growth phenomena at nanoscale the presence of the catalytic particles is fundamental, nevertheless the details of how they define the nanostructure morphology is not well understood. In the present work, we show how the catalytic particle shape is important to determine the morphological symmetries. Our study shows that when both semiaxes of the elliptic catalyst are $\geq (\rho + \Delta)$ the growth of amorphous *binormal* nanospring is energetically favoured through the VLS growing model. So, for $\Delta = 0.5$ and $\rho = 1.0$, and the elliptic catalytic particle with semiaxes 1.5 and 2.0, Fig. 4 shows that the *binormal* nanohelix is clearly favoured energetically. It might be possible to grow an amorphous *normal* nanospring within the VLS model only if the elliptic catalytic particle has its minor semiaxis $< (\rho + \Delta)$. We hope that our analysis will stimulate further theoretical and experimental investigations for growing the various types of helical nanostructures.

This work was partially supported by the FAPESP, CNPq, IMM, IN, THEO-

NANO and FINEP. AFF acknowledges a scholarship from the Brazilian Agency CNPq.

- [1] Iijima S 1991 *Nature* **354** 56.
- [2] Baughman R H, Zakhidov A A and de Heer W A 2002 *Science* **297** 787.
- [3] Ratner D and Ratner M A 2002 *Nanotechnology: A Gentle Introduction to the Next Big Idea* (Upper Saddle River: Pearson Education).
- [4] Samuelson L 2003 *Mater. Today* **6** 22.
- [5] Edelstein A S and Cammarata R C 1996 *Nanomaterials: synthesis, properties and applications* (Bristol: Institute of Physics Publishing).
- [6] Wong K W, Zhou X T, Au F C K, Lai H L, See C S and See S T 1999 *Appl. Phys. Lett.* **75** 2918.
- [7] Gudixsen M S, Laudon L J, Wang J, Smith D C and Lieber C M 2002 *Nature* **415** 617.
- [8] Liu H I, Biegelsen D K, Ponce F A, Johnson N M and Pease R F W 1994 *Appl. Phys. Lett.* **64** 1383.
- [9] Da Fonseca A F, Malta C P and Galvão D S 2006 *J. Appl. Phys.* **99** 094310.
- [10] McIlroy D N, Alkhateeb A, Zhang D, Aston D E, Marcy A C and Norton M G 2004 *J. Phys.: Condens. Matter* **16** R415.
- [11] Tang Y H, Zhang Y F, Wang N, Lee C S, Han X D, Bello I, Lee S T 1999 *J. Appl. Phys.* **85** 7981.
- [12] Zhang H F, Wang C M, Wang L S 2002 *Nano Lett.* **2** 941.
- [13] Amelinckx S, Zhang X B, Bernaerts D, Zhang X F, Ivanov V and Nagy J B 1994 *Science* **265** 635.
- [14] Kong X Y and Wang Z L 2003 *Nano Lett.* **3** 1625.
- [15] Gao P X, Ding Y, Mai W, Hughes W L, Lao C and Wang Z L 2005 *Science* **309** 1700.
- [16] McIlroy D N, Zhang D, Kranov Y and Norton M G 2001 *Appl. Phys. Lett.* **79** 1540.
- [17] Zhang H F, Wang C M, Buck E C and Wang L S 2003 *Nano Lett.* **3** 577.
- [18] Zhang D, Alkhateeb A, Han H, Mahmood H, McIlroy D N and Norton M G 2003 *Nano Lett.* **3** 983.
- [19] Mukhopadhyay K, Porwal D, Ram K and Bhasker Rao K U 2007 *J. Mater. Sci.* **42** 379.
- [20] Wang L, Major D, Paga P, Zhang D, Norton M G and McIlroy D N 2006 *Nanotechnology* **17** S298.
- [21] Veríssimo C, Moshkalyov S A, Ramos A C S, Gonçalves J L, Alves O L and Swart J W 2006 *J. Braz. Chem. Soc.* **17** 1124.
- [22] Wagner R S and Ellis W C 1964 *Appl. Phys. Lett.* **4** 89.
- [23] Goriely A and Shipman P 2000 *Phys. Rev. E* **61** 4508.
- [24] Da Fonseca A F, Malta C P and Galvão D S 2006 *Nanotechnology* **17** 5620.
- [25] Da Fonseca A F, Malta C P and Galvão D S 2007 Elastic Properties of Normal and Binormal Helical Nanowires, in Nanowires and Carbon Nanotubes – Science and Applications, (Mater. Res. Soc. Symp. Proc. 963E, Warrendale, PA, 2007), 0963-Q20-27.
- [26] Gao H, Zhang X, Zhou M, Zhang E and Zhang Z 2006 *Solid State Communications* **140** 455.
- [27] Struik D J 1961 *Lectures on Classical Differential Geometry* (Cambridge: Addison-Wesley) p 1.
- [28] Da Fonseca A F and Galvão D S 2004 *Phys. Rev. Lett.* **92** 175502.